Dentin-derived Inorganic Minerals Promote the Osteogenesis of Bone Marrow-derived Mesenchymal Stem Cells: Potential Applications for Bone Regeneration

Gang Lei
Nanjing Medical University
Yanqiu Wang
Nanjing Medical University
Yan Yu
Nanjing Medical University
Zehan Li
Nanjing Medical University
Jiamin Lu
Nanjing Medical University
Xingyun Ge
Nanjing Medical University
Na Li
Nanjing Medical University
Jinhua Yu (yujinhua@njmu.edu.cn)
Nanjing Medical University https://orcid.org/0000-0003-4874-9910

Research

Keywords: DIM, BMMSCs, MAPK, osteogenic differentiation, bone regeneration

Posted Date: June 12th, 2020

DOI: https://doi.org/10.21203/rs.3.rs-34650/v1

Version of Record: A version of this preprint was published at Stem Cells International on November 19th, 2020. See the published version at https://doi.org/10.1155/2020/8889731.

Abstract

Background Oral and maxillofacial bone loss is highly prevalent among populations and nowadays increased attention has been focused on dentin derivatives as desirable graft materials for bone regeneration. In this study, dentin-derived inorganic minerals (DIM) were fabricated with a high-temperature calcination technique and the effects of DIM on the osteogenic differentiation of bone marrow-derived mesenchymal stem cells (BMMSCs) and the bone formation were elucidated.

Methods The effects of DIM on BMMSCs proliferation, apoptosis capacity were evaluated by CCK-8, flow cytometry and EdU assays. Alkaline phosphatase (ALP) activity detection, ALP staining, alizarin red staining and osteogenic markers expression analysis were performed to investigate the influence of DIM on the osteogenic differentiation of BMMSCs, as well as the relevant signal mechanisms. The model of critical-sized defects in calvarium of rats was constructed for exploring the *in vivo* efficiency of DIM on bone regeneration.

Results Cell viability assays indicated that DIM had no cytotoxicity. BMMSCs cultured with DIM presented a higher level of osteogenic differentiation ability than those in the control group. The activation in ERK and p38 signals was detected in DIM-treated BMMSCs, and both pathways and osteogenic process were suppressed while using ERK inhibitor U0126 and p38 inhibitor SB203580, respectively. Furthermore, the animal experiments revealed that DIM could dramatically enhance new bone formation compared to the control group.

Conclusion All these results demonstrated that DIM could promote BMMSCs osteogenic differentiation via triggering ERK and p38 MAPK signaling pathways and be a novel predictable material for facilitating bone formation.

Background

Oral and maxillofacial bone deficiencies due to congenital malformation, tumor resection, trauma and infection such as periodontitis or periapical inflammation are highly prevalent among populations. Excessive bone loss often results in the spontaneous bone healing failure, thus requiring valid alternatives to conventional treatments for bone repair, such as bone tissue engineering (BTE) [1]. To date, most BTE strategies aim to design a suitable bone graft material for filling the defect volume and providing a supporting substrate by mimicking the extracellular matrix for functional cells migration, proliferation and differentiation [2]. Bone marrow-derived mesenchymal stem cells (BMMSCs), the non-hematopoietic stem cells located in bone marrow, are most readily recruited into the defective site and hold the capacity to turn into multiple cell lineages including adipocytes, chondrocytes and osteoblasts [3]. Faced with bone injury, BMMSCs respond, remove from bone marrow niche into the peripheral circulation and migrate through vascular walls into target tissues, then become the osteoprogenitors that give rise to osteoblasts [4, 5]. The major superiorities of BMMSCs are their higher accessibility, stronger

proliferative capacity and lower antigenicity, enabling the application of them not only in endogenous regeneration of tissues but also in cell transplantation for tissue engineering [3].

Ideal bone graft materials are the key to success in BTE, which should have the following characteristics: highly porous, promotion of stem cell differentiation, non-cytotoxicity and osteoconductivity [6]. In the light of the additional surgery and donor site morbidity of autogenous bone, as well as immunological rejection and spread of diseases of allogeneic bone, it is important to develop artificial bone grafts for repairing oral and maxillofacial bone defects [7]. Previous studies have found that tooth and maxillofacial bone both embryologically originate in the neural crest, sharing identical origin [8]. The composition of tooth, especially dentin, made up of 70% minerals, 20% organics and 10% water, is very close to bone [9]. Based on these similarities, researchers have considered dentin derivatives as novel bone graft materials for reconstructing oral and maxillofacial bone defects. Demineralization, denaturation and freeze-dried technique are the conventional preparation methods of dentin [10, 11]. The osteoinduction property of demineralizaed dentin was first discovered in Urist's report, as evidenced by the process of connective tissues into bone by endochondral ossification under the inducement [12, 13]. In our previous work, dentin non-collagenous proteins (DNCPs) as the major components of deminerliazed dentin, has been proved to promote BMMSCs osteogenic differentiation via MAPK pathways [14].

Dentin-derived inorganic minerals (DIM) are prepared from discarded extracted teeth by denaturing dentin at high temperatures. After calcinations, the organic components of teeth are destructed and the remaining powder consists of inorganics, the major ingredients of which are hydroxyapatite (HA) and tricalcium phosphate (TCP) [15]. The two calcium phosphate has been widely employed in clinic for bone reconstruction with excellent biocompatibility, osteoconduction and similarity to the mineralogical structure of bone [16]. During the bone repair, HA/TCP composite could be biodegraded and osteoblasts could be absorbed well to promote the reconstruction of the defects [17, 18]. Researches showed that HA/TCP ceramic scaffold could make BMMSCs produce new mineralized extracellular matrix and induce hard tissue formation [19]. It was evident that BMMSCs manifested strong osteogenic potential when cultured with β-TCP [20]. Based on these reports, DIM is defined as a material with better osteoconductive property, no immunogenicity and high porosity which aids in adhesion and survival of cells. Studies performed in ovariectomized rats and patients with jaw bone defects demonstrated that tooth powder and plaster of Paris could be mixed as an effective, yet easily manipulable bone substitute material [15, 21]. In another work, calcined tooth powder in combination with silver nanoparticles additives could promote the periodontal ligament stem cells (PDLSCs) differentiate into odontogenesis [22]. Previously, we used DIM to induce human dental pulp stem cells (DPSCs) osteogenic differentiation *in vitro* and have found that the material showed good osteogenic potential [23].

In this research, both *in vitro* cellular experiments and the animal model will be conducted for further exploring DIM efficacy on the osteogenic differentiation capacity of BMMSCs before its clinical use.

Materials And Methods

Material preparation

80 healthy permanent teeth were collected after obtaining patients' informed consent at the Department of Oral and Maxillofacial Surgery of Affiliated Stomatological Hospital of Nanjing Medical University. First, soft tissues, enamel and cementum were removed from the collected teeth. Then successfully separated dentin was calcined using a box furnace at 950℃ with a heating rate of 10 °C min^{-1}, and maintained at 950℃ for 30 min. After that, we let the production cool down naturally to room temperature and ground them into powder. The powder was finally filtered out and collected as dentin-derived inorganic minerals (DIM). X-ray diffraction (XRD) technique was utilized for determining DIM constituents. 20 g DIM was added into 100 mL alpha minimum essential medium (α-MEM, Gibco, Life Technologies, USA) under stirring to form a uniform mixture. The mixture was placed at 37℃ in 5% CO_2 for 5 d, then centrifuged at 400 rpm for 10 min, and the supernatant layer was purified by a 0.22 μm strainer, finally hermetically preserved as mother solution of DIM-CM. In accordance with the concentration of bioceramic extracts studied in documents, the original solution was diluted to 20 mg/mL, 2 mg/mL, 0.2 mg/mL, 20 μg/mL, 2 μg/mL for the following experiments.

Cell isolation and culture

BMMSCs were harvested from 3-week-old male Sprague-Dawley (SD) rats bought from the Animal Core Facility of Nanjing Medical University. In brief, the rats were dissected, separating the femurs and tibias. Then scissors were used to open the marrow cavity and bone marrow was flushed out with 5 mL syringes supplemented with complete medium into the 15 mL centrifuge tubes. After that, the collection was centrifuged at 1000 rpm for 5 min and subsequently resuspended in α-MEM containing 10% fetal bovine serum (FBS, Gibco), 100 g/mL streptomycin and 100 U/mL penicillin. Cells were then inoculated in culture flask and cultured in an incubator with 5% CO_2 at 37 °C. The medium was changed every three days after the initial plating. When reached 80% confluence, cells were amplified by passage culture.

Alkaline phosphatase (ALP) activity and staining

ALP activity assay kit (Jiancheng, Nanjing, China) was used to detect the ALP activity of treated BMMSCs based on the guildines provided by the manufacturer. Cell lysis was obtained with 100 μL 1% TritonX-100 for 30 min followed by the ultrasonication, then added into the testing agents. Finally, the ALP activity was examined using a microplate (Bio-tek, USA). ALP staining was conducted with the NBT/BCIP staining kit (Beyotime, Guangzhou, China). Briefly, the treated BMMSCs were fixed in 4% paraformaldehyde solution for 30 min and then rinsed with PBS twice. Subsequently, cells were stained with ALP premix substrate solution at 37 °C for 30 min away from light.

CCK-8 assay

Cell proliferation was evaluated with the Cell Counting Kit-8 (CCK-8, Dojindo, Kumamoto, Japan) according to the manufacturer's instructions. 1000 cells/well were seeded into 96-well cell culture plates. At a given point in time (1, 3, 5, 7, 9 d), cells were incubated with 10 μL CCK-8 solution for 2 h away from light. The absorbance at a wavelength of 450 nm was calculated with a microplate reader (Bio-tek, USA).

5-Ethynyl-2'-deoxyuridine (EdU) assay

Cell proliferation analysis was carried out with an EdU detection kit (RiboBio, Guangzhou, China). Cells were cultured with 50 μM EdU for 2 h at 37℃, then fixed in 4% paraformaldehyde for 30 min and premeabilized with 0.5% Triton X-100 for 10 min. After that, cells were treated with Apollo® reaction cocktail for 30 min. For nuclear staining, cells were treated with Hoechst 33342 for 30 min and visualized with a fluorescent microscope (Olympus, Tokyo, Japan).

Flow cytometry

Cells were digested by trypsin, resuspended in 4 mL PBS and centrifuged at 1000 rpm for 12 min. Then cells were fixed with 75% precooled ethanol at 4℃ overnight, followed by staining in 1 mL PI. Cell cycle was detected using flow cytometry (BD Biosciences, San Jose, CA) and proliferation index (PI, G2/M + S) in each group was count and compared. For cell apoptosis detection, cells were digested by trypsin, resuspended in 6 mL PBS and centrifuged at 1000 rpm for 6 min twice, then examined with flow cytometry.

Alizarin red staining

Cells mineralization capacity was examined with alizarin red staining. In short, cells were seeded into 12-well plates at a density of 5×10^4 cells per well and incubated for 14 days. Then cells were fixed in 95% ethanol for 1 h. Subsequently, cells were stained with the Alizarin red S solution (pH 4.2, Sigma-Aldrich, USA) for 10 min. The mineralized nodules were observed and photographed under an inverted microscope. For quantification of mineralization, the dye was dissolved using 10% cetylpyridinium chloride (Sigma, UK) for 1 h, then detected by a microplate reader at 540 nm wavelength.

Quantitative real-time polymerase chain reaction (qRT-PCR)

Total RNA was isolated from BMMSCs using TRIzol Reagent (Invitrogen, Carlsbad, CA, USA) and processed into cDNA with the PrimeScript RT Master Mix Kit (TaKaRa Bio, Otsu, Japan). qRT-PCR was conducted by an ABI 7300 Real-Time PCR System (Applied Biosystems, Carlsbad) by mixing cDNA templates, primers (Sangon Biotech, Nanjing, China) and the SYBR Premix Ex Taq kit (TaKaRa Bio). GAPDH was used as the control. The relative primers were displayed below: OCN: forward, 5'-ATTGTGACGAGCTAGCGGAC-3', reverse, 5'-CTGTGCCGTCCATACTTTCG-3', OSX: f, 5'-

GGAGGCACAAAGAAGCCATA-3', r, 5'-GGGAAAGGGTGGGTAGTCAT-3', RUNX2: f, 5'-TTAACGTCAGCAGGAGCAG-3', r, 5’-CTTCACCCCCAGGACCAAG-3', ALP: f, 5'-GGAACGGATCTCGGGGTACA-3', r, 5’-ATGAGTTGGTAAGGCAGGGT-3', OPN: f, 5'-GCGATCGATAGTGCCGAGAA-3', r, 5'-TCGTGGCTCTGATGTTCCAG-3', COL-I: f, 5'-GCAATGCTGAATCGTCCCAC-3', r, 5'-CAGCACAGGCCCTCAAAAAC-3', GAPDH: f, 5'-CACTGAGCATCTCCCTCACAA-3', r, 5'-GTATTCGAGAGAAGGGAGGGCT-3'.

Western Blot

Total proteins were obtained with RIPA lysis buffer (Beyotime). Individual samples (10 μg/lane) were subjected to sodium dodecyl sulfate-polyacrylamide gel electrophoresis (SDS–PAGE) and blotted onto polyvinylidene fluoride (PVDF, Millipore, MA, USA) membranes. The membranes were blocked using 5% BSA and incubated with primary antibodies, then incubated with goat anti-rabbit and mouse secondary antibodies (1:5000, Proteintech, Wuhan, China) for 1 h. The proteins were visualized with a Western Blotting Imaging System (GE Healthcare, USA). The primary antibodies were displayed below: anti-OCN (1:1000, ab93876, Abcam, Cambridge, UK), anti-OSX (1:1000, ab22552, Abcam), anti-RUNX2 (1:1000, ab76956, Abcam), anti-ALP (1:1000, ab95462, Abcam), anti-OPN (1:1000, ab8448, Abcam), anti-COL-I (1:1000, ab34710, Abcam), anti-ERK (1:1000, #4695, Cell Signaling Technology, MA, USA), anti-p-ERK (1:1000, #4370, CST), anti-JNK (1:1000, #9252, CST), anti-p-JNK (1:1000, #9255, CST), anti-p38 (1:1000, #8690, CST), anti-p-p38 (1:1000, #4511, CST) and anti-GAPDH (1:1000, AP006, Bioworld, China).

Animal experiments

Calvarial defect models were performed in 24 male SD rats at 8 weeks of age bought from the Animal Core Facility of Nanjing Medical University. The rats were given an intraperitoneal injection of 10% chloral hydrte to anaesthetize them: the dosage was 0.4 mL/100 g body weight. Then a sagittal incision (length of around 2 cm) was created on the scalp of the rats. Thereafter,the soft tissue covering the calvarium was sharply divided and pushed gently into the lateral. Furthermore, two 5-mm-diameter bilateral bone defects were drilled on the calvarias using a portable dental turbine (Xin he an, Wu han, China) and a circular trephine. Finally, 5 mg DIM powder was subsequently implanted into the bone defect on the left side while the right side was left empty (control). The rats were separated into 3 groups at random: 4-week implantation group, 8-week implantation group and 12-week implantation group, respectively. Post-operative antibiotic therapy was then provided by intramuscular administration of 2×10^5U/d penicillin for 3 days. The rats were euthanized after 4, 8, 12 weeks. The calvarias were harvested and analyzed with Micro-CT assay and histological analysis. The experiments were approved by the protocols of the Institutional Animal Care and Use Committee (IACUC) of Nanjing Medical University (IACUC-1703024).

Microcomputed tomography (Micro-CT) assay

After 4, 8, 12 weeks of surgery, the rats were sacrificed and the calvarias were harvested, followed by fixation in 4% paraformaldehyde, then examined with a Scanco vivaCT 80 scanner (Scanco Medical AG, Bruttisellen, Switzerland) referring to the settings: 15.6 μm resolution at 55 kV and 145 μA. Three-dimension (3D) structures of samples were reconstructed with system software. The bone parameters of the samples including bone mineral density (BMD) and bone volume fraction (bone volume/total volume, BV/TV) were also calculated.

Histological analysis

Calvarias were fixed in 10% neutral formalin for 48 h, then decalcified in 20% EDTA for 2 months. Thereafter, the specimens were embedded in paraffin. 5-μi-thick slices were sectioned and stained with hematoxylin-eosin (H&E) and Masson's trichrome, then fixed with neutral balsam and analyzed under a microscope (Leica, Wetzlar, Germany).

Statistical analysis

Each experiment was performed at least in triplicate. The data were presented as the mean ± SD. Statistical analyses were evaluated with SPSS software 16.0 using Student's *t*-test or one-way analysis of variance (ANOVA). P values < 0.05 were considered statistically significant.

Results

2 mg/mL is the optimal inducement concentration of DIM

To study DIM effects on the osteogenesis of BMMSCs, we prepared DIM powder and made extracting liquid of that, meanwhile we isolated and cultured BMMSCs. XRD was conducted to analyze DIM composition. XRD pattern of DIM was exhibited in Fig. 1D. The results showed that DIM was mainly composed of HA and TCP with a ratio of 97.6:2.4. The calcium to phosphorus ratio was 1.66:1. Primary BMMSCs demonstrated a typical short rod-like or spindle-shaped morphology (Fig. 1A) and hemocytes decreased in number (Fig. 1B). BMMSCs in passage 3 were uniform and had the spindle-shaped appearance (Fig. 1C). The optimal concentration of DIM for inducing BMMSCs osteogenic differentiation was determined with ALP activity detection and ALP staining. As illustrated in Fig. 1E, F, ALP activity and ALP positive staining cells both increased when BMMSCs were induced with 2 mg/mL DIM, which suggested that 2 mg/mL is the best inducement concentration of DIM.

DIM has no effect on BMMSCs proliferation and apoptosis

CCK-8, EdU, and flow cytometry assays were carried out for testing the proliferation of DIM-treated BMMSCs. As shown in Fig. 2A, there was no significant difference in cell proliferation between DIM group and the control group. Furthermore, the results of EdU assay indicated that the number of EdU-positive

cells were same in DIM group and the control group (Fig. 2B, C). Moreover, flow cytometry analysis of the cell cycle distribution showed that there was no significant difference in PI values ($S + G_2M$) between DIM-treated BMMSCs and the control group (Fig. 2D, E). Taken together, these data suggested that DIM had no effect on BMMSCs proliferation. Flow cytometry was also used to evaluate the situation of cell apoptosis in the presence of DIM. The results showed that there was no significant difference in cell apoptotic rate in DIM-treated BMMSCs relative to the control group, as represented in Fig. 2F, G.

DIM promotes BMMSCs osteogenic differentiation *in vitro*

To explore the role of DIM on the osteogenic differentiation of BMMSCs, ALP activity detection and ALP staining was first performed as cells were incubated with DIM for 5 days. As Fig. 3A showed, compared with the control group, there were more ALP positive staining cells in DIM group. Besides, DIM-treated BMMSCs exhibited the higher ALP activity compared to the control (Fig. 3B). Alizarin red staining was carried out to estimate the mineral deposition of the extracellular matrix produced by BMMSCs. The results showed that DIM leaded to a notable increase in the number of calcified nodules in comparison with the control group on the 14th day of cell culture (Fig. 3C, D). Furthermore, the expression levels of osteogenic markers (OCN, OSX, RUNX2, ALP, OPN and COL-1) were determined with qRT-PCR and western blot when BMMSCs were incubated with DIM for 3 and 7 days. We found in the presence of DIM, mRNA and protein expression levels of these markers were elevated in comparison to those in the control group on the 3th and 7th day, respectively. Moreover, expression levels on the 7th day were obviously higher than those on the 3th day (Fig. 3E, F, G). All the corresponding data showed that DIM could promote BMMSCs osteogenic differentiation.

DIM functions in BMMSCs osteogenic differentiation via activating ERK and p38 MAPK pathways

In order to evaluate whether DIM exerted effects on MAPK pathway, MAPK-associated protein expression was detected with western blot at 0, 15, 30 and 60 min. As displayed in Fig. 4A, p-ERK and p-p38 expression reached its maximum at 15 min, then gradually declined. p-JNK was nearly not expressed from 0 to 60 min. Figure 4B quantitatively showed that p-ERK/ERK and p-p38/p38 were up-regulated at 15 min and then dropped, while there was no remarkable difference in the p-JNK/JNK proportion from 0 to 60 min. When MAPK pathway inhibitors (ERK inhibitor U0126, JNK inhibitor SP600125 and p38 inhibitor SB203580) were used respectively, the phosphorylation degree of p-ERK in DIM + U0126 group as well as p-p38 in DIM + SB203580 group reduced apparently in comparison to that in DIM group at 15 min. Meanwhile, the expression level of p-JNK had no change in DIM + SP600125 group compared to that in DIM group (Fig. 4C). Quantitative analysis showed the same tendencies (Fig. 4D). After DIM-treated BMMSCs were cultured with ERK or p38 inhibitors separately for 7 d, the expression of osteogenic markers (OCN, OSX, RUNX2, ALP, OPN and COL-I) were down-regulated in comparison to DIM group, and had no significant difference as compared with that in the control group, indicating that DIM effects were

blocked. (Fig. 4E, F, G). ALP staining showed that the ALP positive cells in DIM group on the 5th day were more than the ones in DIM + U0126 or DIM + SB203580 group (Fig. 4H). These data suggested that DIM functioned in BMMSCs osteogenic differentiation via activating ERK and p38 MAPK pathways.

DIM promotes BMMSCs osteogenesis *in vivo*

All rats recovered with no complication such as infection, bleeding and so on. The bone regeneration within calvarial defects was observed and analyzed by Micro-CT at 4, 8, 12 weeks after implantation. 3D reconstruction results as shown in Fig. 5D suggested that at 4 weeks, only small amount of newly formed bone was found in the peripheral part of the bone defect in DIM group while no bone formation in the control group. At 8 weeks, little new bone was observed in the control group which is much less than that in DIM group. At 12 weeks, there was a lot of new bone formation growing in the central part of the bone defect in DIM group and still major bone defects in the control group. Meanwhile, the DIM transplantation degraded and was not obvious. The higher BV/TV and BMD values of new bone were reached in DIM group in comparison to the control group at 4, 8 and 12 weeks (Fig. 5B, C). Histological analysis of the harvested calvarias from all groups further verified the significant new bone formation in DIM group, consistent with results of Micro-CT. As shown in Fig. 6A, B, at 4 weeks, the bone defect in DIM group was mainly filled with residual DIM and plenty fiber network structures of regularly array were observed. At 8 weeks, new bone was formed across DIM in bone defects (Fig. 6C, D). At 12 weeks, the bone defect treated with DIM was almost completely replaced with reticulated bone and tabular bone (Fig. 6E, F).

Discussion

Repairing and reconstructing oral and maxillofacial bone defects is still full of challenge. Tissue engineering strategies rely mostly on a scaffold composed of osteoconduction and osteoinduction factors, which will allow attachment, growth and differentiation of MSCs and accelerate regeneration of the bone structure [24]. DIM has been proved to be biocompatible and possesses the osteoconductive property [25]. Kim et al. [26] has reported that DIM featured good osteoinductivity in animal experiments. Our prior work has shown that DIM could promote the osteogenic differentiation of human DPSCs [23]. However, DIM efficacy on the osteogenesis capacity of BMMSCs has not yet been studied.

In this study, DIM was obtained and we demonstrated that this material induced the *in vitro* osteogenic differentiation of BMMSCs and promoted bone formation in an experimental rat model of calvaria defect. XRD technique was conducted to examine composition characteristics of DIM. The results showed that characteristic peak of DIM is similar with that of HA/TCP, which suggested that DIM mainly consist of HA and TCP. Further analysis revealed that HA to TCP ratio is 97.6:2.4 and the calcium to phosphorus ratio is 1.66:1, near to that of human bone. Numerous researches have shown that the ions (such as silicon, calcium, sodium, phosphorous, etc.) play an important role in cell growth and metabolism, also activate some osteogenic related genes and promote the mineralization of extracelluar matrix [27]. Calcium channel of lysosomes are necessary in the process of signal transduction during bone remodeling and

maintaining bone homeostasis [28]. It has been proved that calcium ions could promote bone formation in a subperiosteal space [29]. Some studies indicate that the mechanism of calcium phosphate materials in repairing bone defects were based on their released measurable amounts of calcium and phosphorous, which could lead to the apatite reprecipitating onto the material surface and facilitate the bone formation [30]. Rashid has reported that successful bone regeneration with DIM was attributed to localised increased calcium concentration, upregulating the expression level of osteogenic markers (OPN and BMP2) [31].

Generally, to simplify the research work regarding bioceramic materials [32], we made extracting liquid of DIM and confirmed that DIM at a concentration of 2 mg/mL had the optimum inducement capacity for BMMSCs osteogenic differentiation, which can be used for further experiments. The results of CCK-8, EdU and flow cytometry assays showed that DIM had no effect on BMMSCs proliferation and apoptosis, suggesting that DIM exhibited good cytobiocompatibility.

As described previously, the early phases in the differentiation of BMMSCs towards osteoblasts occur from day 5 to 14 in incubation and is characterized by ALP expression [33]. The maturation and mineralization of the extracellular matrix produced during osteoblastic differentiation take places from day 14 to 28 in incubation and alizarin red staining is the most explored parameter for research [34]. While treated with DIM for 5 days, BMMSCs expressed high level of ALP activity compared to the control group. Meanwhile, the amount of ALP positive staining cells in DIM group was obviously much than that in the control group. In alizarin red staining, DIM group presented an up-regulation in calcium nodules and the quantification of calcium contents revealed that DIM-treated BMMSCs showed higher amounts of calcium than the control group. Based on these findings, we hypothesized that DIM could promote BMMSCs osteogenic differentiation. To further validate the speculation, the expression of related osteogenic markers (OCN, ALP, OPN and COL-I) and transcription factors (RUNX2 and OSX) was detected. OPN and OCN are both downstream of RUNX2, representing the late stage of the osteogenesis [35]. COL-I, the main organic component of bone, provides specific functions of scaffold structure for the differentiating cells adhesion [36]. RUNX2 and OSX are vital transcriptional factors associated with the osteoblast differentiation, [37]. We found the above markers were highly expressed in DIM-induced BMMSCs on the 3th and 7th day, as indicated by western blot and qRT-PCR. Therefore, we showed that 2 mg/mL DIM could positively regulate the osteogenic differentiation capacity of BMMSCs.

Mechanisms of DIM in regulating the promotion of BMMSCs osteogenic activities needed to be explored. It's well known that a number of signaling pathways contribute to osteogenic programs of MSCs, such as mitogen-activated protein kinase (MAPK), Notch and NF-κB pathways [38]. MAPK superfamily, including extracellular signal-regulated kinase (ERK), c-Jun N-terminal kinase (JNK) and p38, is one of the most thoroughly studied signal transduction systems. It participates in multiple cellular responses to stimulus of inside or outside the body, like proliferation, differentiation and cell death [39]. ERK and p38 MAPKs play a role in the osteoblast differentiation by directly phosphorylating the master transcriptional factor RUNX2 [40]. In the former exploring studies, we have found ERK and p38 MAPKs are related to the osteogenesis of BMMSCs [14]. Some studies have demonstrated that the biomedical ceramics and their

released ions could promote MSCs osteogenic differentiation by activating MAPK signals. For example, Xia et al. observed that ERK and p38 MAPKs were activated in the osteogenesis process of BMMSCs while cultured on HA bioceramic scaffolds [41]. In addition, extracellular calcium ions could bond the calcium-sensing receptors (CSR) to start the cascade reactions of the ERK MAPK pathway and induce the bone formation [42]. Calmodulin-dependent protein kinase II (CaMKII)/TAK1 could autophosphorylate in calcium mediated signal transduction system then activate p38 MAPK to induce cell activities [43, 44]. In this study, the phosphorylation state of MAPK pathway was tested in BMMSCs when stimulated to differentiate by DIM and we found that ERK and p38 became phosphorylated. While the pathways were treated with their corresponding inhibitors during cell culture with DIM, ERK and p38 were suppressed, and the augmentation of BMMSCs osteogenic differentiation capacity (ALP staining and osteogenic markers expression level) was decreased to levels which were not significantly different from the control. Therefore, DIM were proved to promote BMMSCs osteogenic differentiation by upmodulating osteogenic markers by requiring the activation of ERK and p38 MAPKs. It is speculated that calcium ions released from DIM may determine the activation of ERK and p38 MAPKs by binding CSR or CaMKII.

These *in vitro* experimental results urged us to evaluate the osteogenesis potential of DIM *in vivo*. To access the bone repairing ability of graft materials, the natural bone healing in experimental bone defects should be inhibited. The critical-sized defect is known to be a non-united tissue defect which will never spontaneously heal [45]. In this study, the model of critical-sized defects in calvarium of rats (5 mm in diameter) was established to observe new bone formation after DIM placement [46]. Preferred observation intervals (4, 8, 12 weeks) were assigned to access bone formation (4 weeks), and to access bone maturation, side effects as well as absorption of DIM (8, 12 weeks). After the procedure, all rats recovered without immunological rejection and complications such as infection, hemorrhage et al, occurred, indicating the implanted material had good biocompatibility with cells. To observe and quantify the state of new bone formation, Micro-CT and histological examinations were carried out on the samples at the different time points post-surgery. Histological analysis showed that DIM material was intertwined by plenty of reticular fiber-like network structures, and over time, these structures were gradually mineralized and some of them became reticulated bone. At 12 weeks, bulk bone was formed and the fiber-like structures were completely absorbed. Our results suggested that DIM could induce the new bone generation in the critical-sized defects over time, meanwhile DIM was gradually degraded to provide space for BMMSCs differentiation. The better biodegradation than artificial HA brings in favorable clinical prospects for DIM. Combined with the *in vitro* findings, the underlying mechanism of DIM function might rely on the osteoinductive and osteoconductive signals released by DIM. DIM could create a microenvironment in which calcium and phosphorus reached appropriate concentrations to activate ERK and p38 MAPK pathways, thus induce BMMSCs differentiation into osteoblasts, also serve as a good scaffold material for adhesion, working of cells as well as the deposition of newly generated bone. Therefore, it was safe to conclude that the use of DIM did lead to the osteogenesis of BMMSCs and could repair the bone defects in rat critical-sized calvarial defect models.

Conclusion

We demonstrated for the first time, DIM could promote the osteogenic differentiation capacity of BMMSCs via activating ERK and p38 MAPK signaling pathways. In addition, DIM could effectively enhance the bone regeneration as a unique scaffold. Our studies creatively proposed that DIM could be a promising candidate bone graft material capable of mediating efficient bone formation in oral and maxillofacial bone defects.

Abbreviations

DIM: dentin-derived inorganic mineral; **BMMSCs**: bone marrow-derived mesenchymal stem cells; **ALP**: Alkaline phosphatase; **BTE**: bone tissue engineering; **DNCPs**: dentin non-collagenous proteins; **HA**: hydroxyapatite; **TCP**: tricalcium phosphate; **PDLSCs**: periodontal ligament stem cells; **DPSCs**: human dental pulp stem cells; **α-MEM**: alpha minimum essential medium; **SD**: Sprague Dawley; **FBS**: fetal bovine serum; **CCK-8**: Cell Counting Kit-8; **EdU**: 5-Ethynyl-2'-deoxyuridine; **PI**: proliferation index; **qRT-PCR**: quantitative real-time polymerase chain reaction; **SDS–PAGE**: sulfate-polyacrylamide gel electrophoresis; **PVDF**: polyvinylidene fluoride; **Micro-CT**: microcomputed tomography; **3D**: three-dimension; **BMD**: bone mineral density; **BV**: bone volume; **TV**: total volume; **H&E**: hematoxylin-eosin; **ANOVA**: analysis of variance; **MAPK**: mitogen-activated protein kinase; **ERK**: extracellular signal-regulated kinase; **JNK**: c-Jun N-terminal kinase; **CSR**: calcium-sensing receptor.

Declarations

Availability of data and material

The datasets generated and/or analyzed during the current study are available from the corresponding author on reasonable request. All data generated or analyzed during this study are included in this published article.

Acknowledgements

Not applicable.

Funding

This work was supported by National Natural Science Foundation of China (81873707, 81900962), Medical Talent Project of Jiangsu Province (ZDRCA2016086), the Priority Academic Program Development of Jiangsu Higher Education Institutions (PAPD, 2018-87), SuYan Research & Development Funds for Intelligent Health Science & Technology Innovation (NMU-SY201804), and Science and Technology Development Project of Jiangsu Province (BE2017731).

Authors' contributions

Lei Gang and Yanqiu Wang conceived and designed the study, collected and assembled data and wrote the manuscript. These two authors contributed equally to this work. Yan Yu performed data analysis and interpretation. Zehan Li, Jiamin Lu, Xingyun Ge and Na Li edited the paper. Jinhua Yu supervised the overall study design and provided financial support. All authors read and approved the manuscript.

Ethics approval and consent to participate

Teeth were collected after obtaining patients' informed consent at the Department of Oral and Maxillofacial Surgery of Affiliated Stomatological Hospital of Nanjing Medical University. All animal experiments were approved by the protocols of the Institutional Animal Care and Use Committee (IACUC) of Nanjing Medical University (IACUC-1703024).

Consent for publication

Not applicable.

Competing interests

The authors declare that they have no competing interests.

References

1. Borciani G, Montalbano G, Baldini N, Cerqueni G, Vitale-Brovarone C, Ciapetti G. Co-culture systems of osteoblasts and osteoclasts: Simulating in vitro bone remodeling in regenerative approaches. Acta Biomater. 2020;108:22-45.
2. Oryan A, Alidadi S, Moshiri A, Maffulli N. Bone regenerative medicine: classic options, novel strategies, and future directions. J Orthop Surg Res. 2014;9:18.
3. Xiao Y, Mareddy S, Crawford R. Clonal characterization of bone marrow derived stem cells and their application for bone regeneration. Int J Oral Sci. 2010;2:127-35.
4. Fong EL, Chan CK, Goodman SB. Stem cell homing in musculoskeletal injury. Biomaterials. 2011;32:395-409.
5. Chen FM, Wu LA, Zhang M, Zhang R, Sun HH. Homing of endogenous stem/progenitor cells for in situ tissue regeneration: Promises, strategies, and translational perspectives. Biomaterials. 2011;32:3189-209.
6. Zadpoor AA. Bone tissue regeneration: the role of scaffold geometry. Biomater Sci. 2015;3:231-45.

7. Rogers GF,Greene AK. Autogenous bone graft: basic science and clinical implications. J Craniofac Surg. 2012;23:323-7.
8. Yoshida T, Vivatbutsiri P, Morriss-Kay G, Saga Y, Iseki S. Cell lineage in mammalian craniofacial mesenchyme. Mech Dev. 2008;125:797-808.
9. Linde A,Goldberg M. Dentinogenesis. Crit Rev Oral Biol Med. 1993;4:679-728.
10. Kim YK, Lee J, Um IW, Kim KW, Murata M, Akazawa T, et al. Tooth-derived bone graft material. J Korean Assoc Oral Maxillofac Surg. 2013;39:103-11.
11. Tabatabaei FS, Tatari S, Samadi R, Moharamzadeh K. Different methods of dentin processing for application in bone tissue engineering: A systematic review. J Biomed Mater Res A. 2016;104:2616-27.
12. Bang G,Urist MR. Bone induction in excavation chambers in matrix of decalcified dentin. Arch Surg. 1967;94:781-9.
13. Yeomans JD,Urist MR. Bone induction by decalcified dentine implanted into oral, osseous and muscle tissues. Arch Oral Biol. 1967;12:999-1008.
14. Yu Y, Wang L, Yu J, Lei G, Yan M, Smith G, et al. Dentin matrix proteins (DMPs) enhance differentiation of BMMSCs via ERK and P38 MAPK pathways. Cell Tissue Res. 2014;356:171-82.
15. Kim SG, Yeo HH, Kim YK. Grafting of large defects of the jaws with a particulate dentin-plaster of paris combination. Oral Surg Oral Med Oral Pathol Oral Radiol Endod. 1999;88:22-5.
16. Rezwan K, Chen QZ, Blaker JJ, Boccaccini AR. Biodegradable and bioactive porous polymer/inorganic composite scaffolds for bone tissue engineering. Biomaterials. 2006;27:3413-31.
17. Wang Y, Yang X, Gu Z, Qin H, Li L, Liu J, et al. In vitro study on the degradation of lithium-doped hydroxyapatite for bone tissue engineering scaffold. Mater Sci Eng C Mater Biol Appl. 2016;66:185-192.
18. Kamalaldin N, Jaafar M, Zubairi SI, Yahaya BH. Physico-Mechanical Properties of HA/TCP Pellets and Their Three-Dimensional Biological Evaluation In Vitro. Adv Exp Med Biol. 2019;1084:1-15.
19. Mastrogiacomo M, Papadimitropoulos A, Cedola A, Peyrin F, Giannoni P, Pearce SG, et al. Engineering of bone using bone marrow stromal cells and a silicon-stabilized tricalcium phosphate bioceramic: evidence for a coupling between bone formation and scaffold resorption. Biomaterials. 2007;28:1376-84.
20. Wang F, Zhou Y, Zhou J, Xu M, Zheng W, Huang W, et al. Comparison of Intraoral Bone Regeneration with Iliac and Alveolar BMSCs. J Dent Res. 2018;97:1229-1235.
21. Kim BK, Kim SG, Kim SY, Lim SC, Kim YK. A comparison of bone generation capability in rabbits using tooth ash and plaster of Paris with platelet-rich plasma or fibrin sealant. Oral Surg Oral Med Oral Pathol Oral Radiol Endod. 2010;110:e8-14.
22. Li X, Liao D, Sun G, Chu H. Odontogenesis and neuronal differentiation characteristics of periodontal ligament stem cells from beagle dog. J Cell Mol Med. 2020;24:5146-5151.

23. Wu J, Li N, Fan Y, Wang Y, Gu Y, Li Z, et al. The Conditioned Medium of Calcined Tooth Powder Promotes the Osteogenic and Odontogenic Differentiation of Human Dental Pulp Stem Cells via MAPK Signaling Pathways. Stem Cells Int. 2019;2019:4793518.
24. Giannoudis PV, Einhorn TA, Marsh D. Fracture healing: the diamond concept. Injury. 2007;38 Suppl 4:S3-6.
25. Skoglund A, Hising P, Young C. A clinical and histologic examination in humans of the osseous response to implanted natural bone mineral. Int J Oral Maxillofac Implants. 1997;12:194-9.
26. Su-Gwan K, Hak-Kyun K, Sung-Chul L. Combined implantation of particulate dentine, plaster of Paris, and a bone xenograft (Bio-Oss) for bone regeneration in rats. J Craniomaxillofac Surg. 2001;29:282-8.
27. Meka SRK, Agarwal V, Chatterjee K. In situ preparation of multicomponent polymer composite nanofibrous scaffolds with enhanced osteogenic and angiogenic activities. Mater Sci Eng C Mater Biol Appl. 2019;94:565-579.
28. Erkhembaatar M, Gu DR, Lee SH, Yang YM, Park S, Muallem S, et al. Lysosomal Ca(2+) Signaling is Essential for Osteoclastogenesis and Bone Remodeling. J Bone Miner Res. 2017;32:385-396.
29. Stevens MM, Marini RP, Schaefer D, Aronson J, Langer R, Shastri VP. In vivo engineering of organs: the bone bioreactor. Proc Natl Acad Sci U S A. 2005;102:11450-5.
30. Priya A, Nath S, Biswas K, Basu B. In vitro dissolution of calcium phosphate-mullite composite in simulated body fluid. J Mater Sci Mater Med. 2010;21:1817-28.
31. Rashid F, Shiba H, Mizuno N, Mouri Y, Fujita T, Shinohara H, et al. The effect of extracellular calcium ion on gene expression of bone-related proteins in human pulp cells. J Endod. 2003;29:104-7.
32. Lu J, Li Z, Wu X, Chen Y, Yan M, Ge X, et al. iRoot BP Plus promotes osteo/odontogenic differentiation of bone marrow mesenchymal stem cells via MAPK pathways and autophagy. Stem Cell Res Ther. 2019;10:222.
33. Halling Linder C, Ek-Rylander B, Krumpel M, Norgard M, Narisawa S, Millan JL, et al. Bone Alkaline Phosphatase and Tartrate-Resistant Acid Phosphatase: Potential Co-regulators of Bone Mineralization. Calcif Tissue Int. 2017;101:92-101.
34. Birmingham E, Niebur GL, Mchugh PE, Shaw G, Barry FP, Mcnamara LM. Osteogenic differentiation of mesenchymal stem cells is regulated by osteocyte and osteoblast cells in a simplified bone niche. Eur Cell Mater. 2012;23:13-27.
35. Tsao YT, Huang YJ, Wu HH, Liu YA, Liu YS, Lee OK. Osteocalcin Mediates Biomineralization during Osteogenic Maturation in Human Mesenchymal Stromal Cells. Int J Mol Sci. 2017;18.
36. Lindahl K, Barnes AM, Fratzl-Zelman N, Whyte MP, Hefferan TE, Makareeva E, et al. COL1 C-propeptide cleavage site mutations cause high bone mass osteogenesis imperfecta. Hum Mutat. 2011;32:598-609.
37. Franceschi RT, Ge C, Xiao G, Roca H, Jiang D. Transcriptional regulation of osteoblasts. Ann N Y Acad Sci. 2007;1116:196-207.

38. Wang Y, Zhou Y, Jin L, Pang X, Lu Y, Wang Z, et al. Mineral trioxide aggregate enhances the osteogenic capacity of periodontal ligament stem cells via NF-kappaB and MAPK signaling pathways. J Cell Physiol. 2017.
39. Payne KA, Meszaros LB, Phillippi JA, Huard J. Effect of phosphatidyl inositol 3-kinase, extracellular signal-regulated kinases 1/2, and p38 mitogen-activated protein kinase inhibition on osteogenic differentiation of muscle-derived stem cells. Tissue Eng Part A. 2010;16:3647-55.
40. Thouverey C,Caverzasio J. Focus on the p38 MAPK signaling pathway in bone development and maintenance. Bonekey Rep. 2015;4:711.
41. Xia L, Lin K, Jiang X, Xu Y, Zhang M, Chang J, et al. Enhanced osteogenesis through nano-structured surface design of macroporous hydroxyapatite bioceramic scaffolds via activation of ERK and p38 MAPK signaling pathways. J Mater Chem B. 2013;1:5403-5416.
42. Li M, He P, Wu Y, Zhang Y, Xia H, Zheng Y, et al. Stimulatory effects of the degradation products from Mg-Ca-Sr alloy on the osteogenesis through regulating ERK signaling pathway. Sci Rep. 2016;6: 32323.
43. Chen S, Xu Y, Xu B, Guo M, Zhang Z, Liu L, et al. CaMKII is involved in cadmium activation of MAPK and mTOR pathways leading to neuronal cell death. J Neurochem. 2011;119:1108-18.
44. Endale M, Kim TH, Kwak YS, Kim NM, Kim SH, Cho JY, et al. Torilin Inhibits Inflammation by Limiting TAK1-Mediated MAP Kinase and NF-kappaB Activation. Mediators Inflamm. 2017;2017:7250968.
45. Gosain AK, Santoro TD, Song LS, Capel CC, Sudhakar PV, Matloub HS. Osteogenesis in calvarial defects: contribution of the dura, the pericranium, and the surrounding bone in adult versus infant animals. Plast Reconstr Surg. 2003;112:515-27.
46. Ferreira LB, Bradaschia-Correa V, Moreira MM, Marques ND, Arana-Chavez VE. Evaluation of bone repair of critical size defects treated with simvastatin-loaded poly(lactic-co-glycolic acid) microspheres in rat calvaria. J Biomater Appl. 2015;29:965-76.

Figures

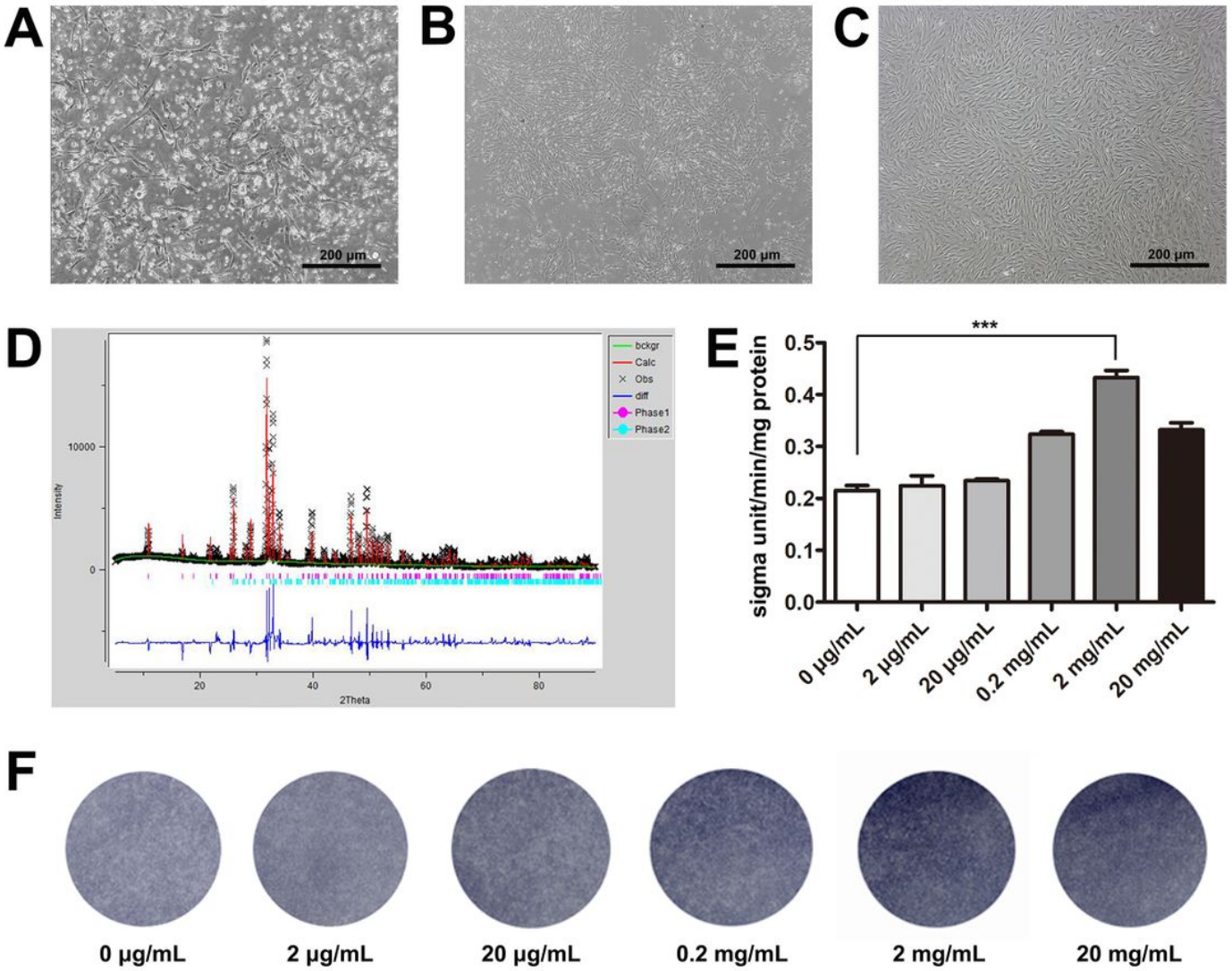

Figure 1

Optimal concentration of DIM for the following experiments (A, B) Primary BMMSCs. Scale bars=200 μm. (C) BMMSCs in passage 3. Scale bars=200 μm. (D) XRD pattern of DIM. (E) ALP activity detection after BMMSCs were treated with 0 μg/mL, 2 μg/mL, 20 μg/mL, 200μg/mL, 2 mg/mL and 20 mg/mL DIM on the 3th day, respectively. ***P<0.001. (F) ALP staining after BMMSCs were treated with 0 μg/mL, 2 μg/mL, 20 μg/mL, 200μg/mL, 2 mg/mL and 20 mg/mL DIM on the 3th day, respectively.

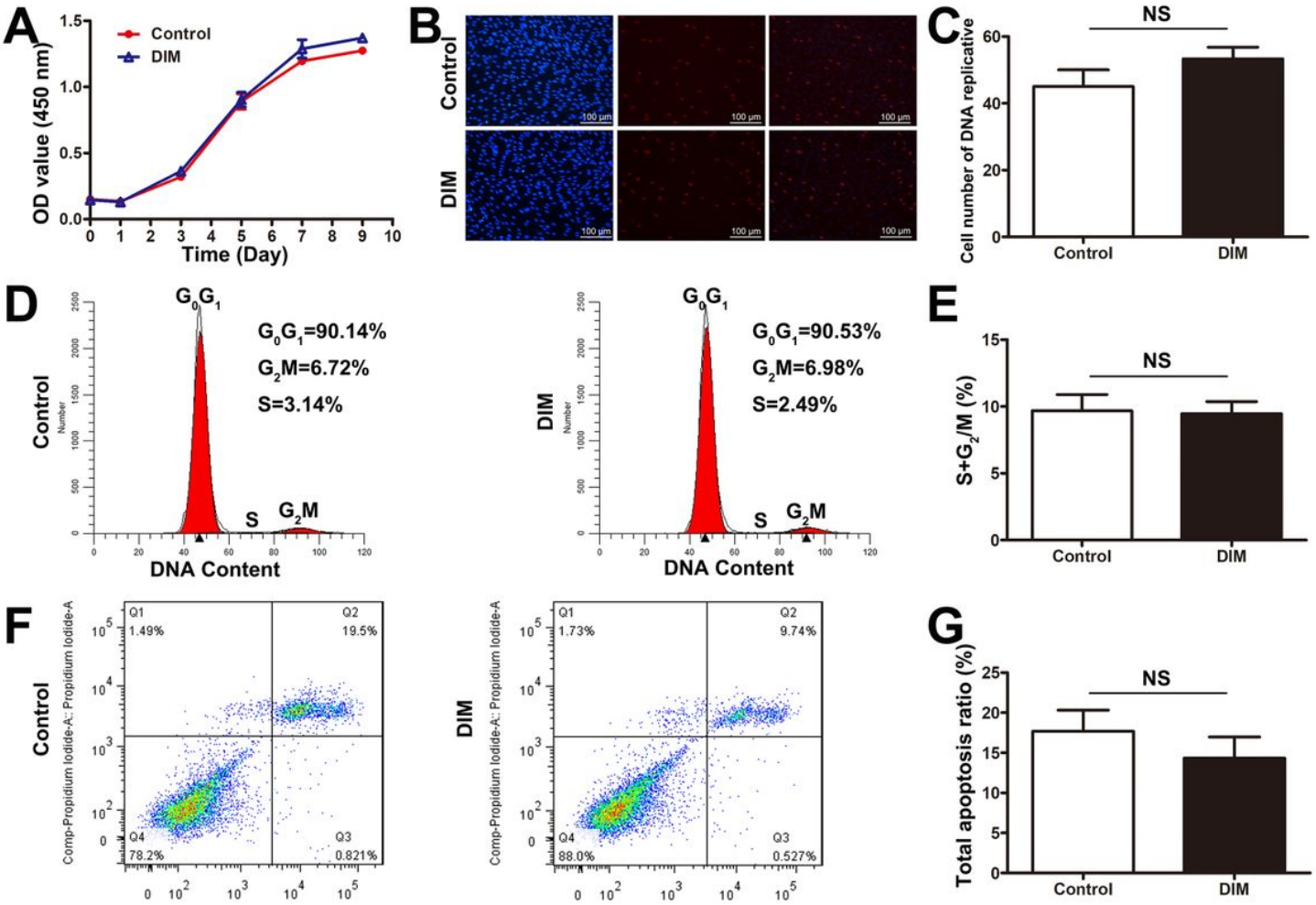

Figure 2

Effects of DIM on BMMSCs proliferation and apoptosis (A) CCK-8 assay was performed to measure the effect of DIM on the proliferation of BMMSCs at the indicated time points. (B) EdU-positive cells under microscope. Scale bars=100 μm. (C) Quantification of EdU assay. P>0.05. (D) Flow cytometry determination of proportion of BMMSCs in distinct cell-cycle phases. (E) Quantitative analysis of (D). P>0.05. (F) Flow cytometry was performed to measure cell apoptosis of BMMSCs treated with DIM. (G) Quantitative analysis of (F). P>0.05.

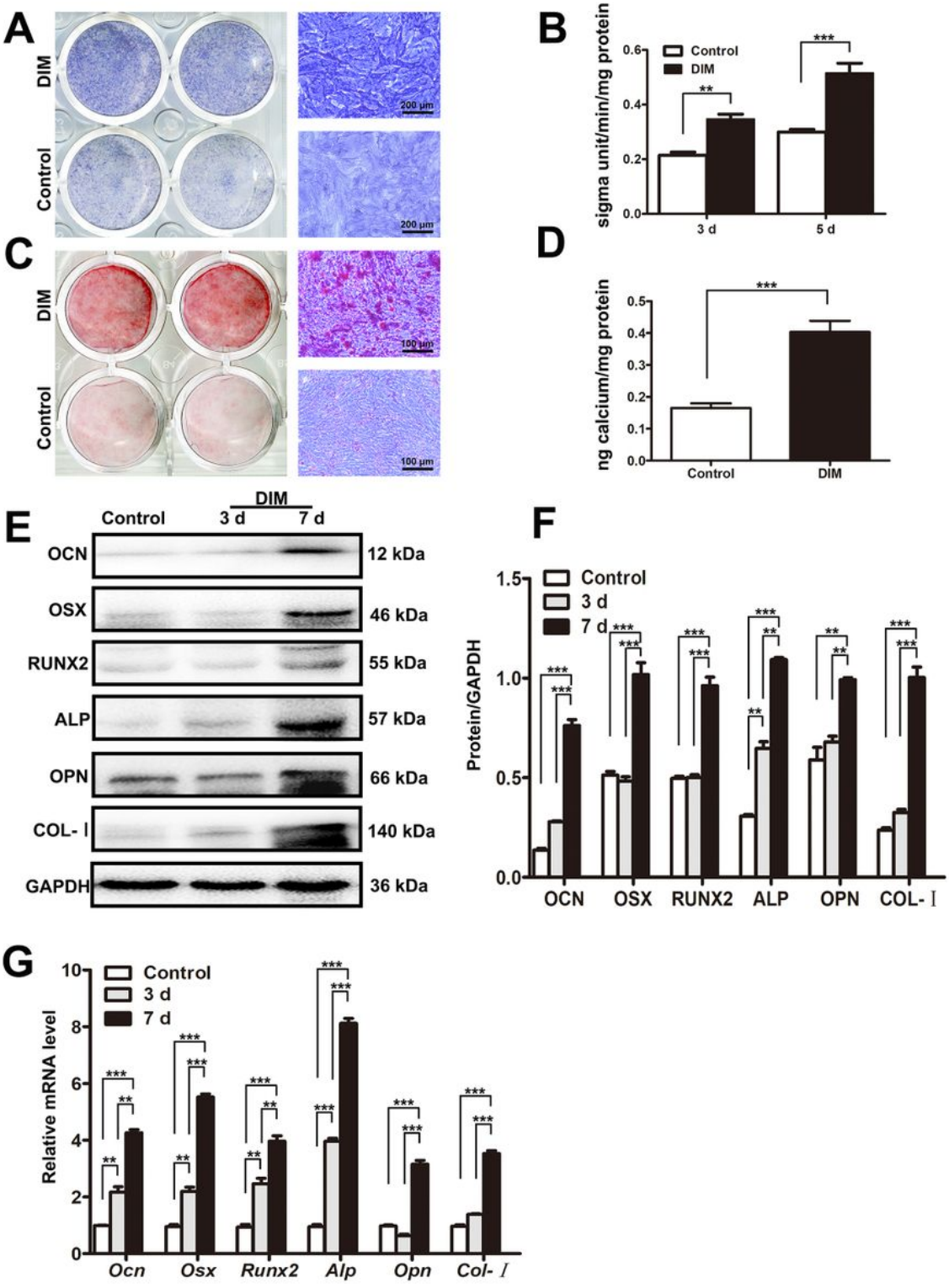

Figure 3

Effects of DIM on BMMSCs osteogenic differentiation (A) ALP staining after BMMSCs were treated with 2 mg/mL DIM on the 5th day. Scale bars=100 μm. (B) ALP activity after BMMSCs were treated with 2 mg/mL DIM on the 5th day. **P<0.01, ***P<0.001. (C) Alizarin red staining showed calcium deposition after 14 days of culture. Scale bars=200 μm. (D) Quantification of (C). ***P<0.001. (E) Protein expression levels of OCN, OSX, RUNX2, ALP, OPN and COL-I were determined with western blot. (F) Quantification of

(E). **P<0.01, and ***P<0.001. (G) mRNA expression levels of OCN, OSX, RUNX2, ALP, OPN and COL-I were determined with qRT-PCR. **P<0.01, and ***P<0.001.

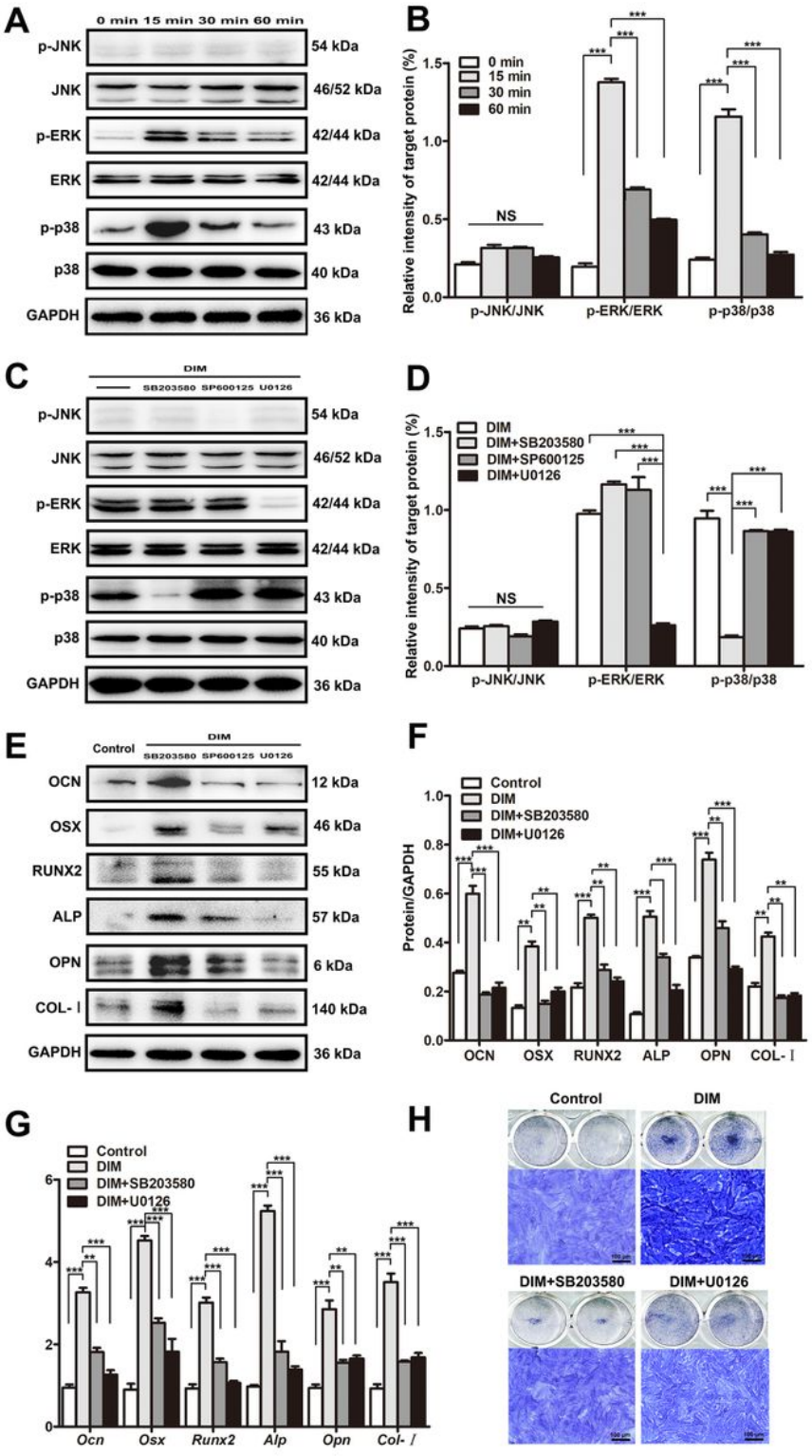

Figure 4

Effects of DIM on ERK and P38 MAPK pathways involved in BMMSCs osteogenic differentiation (A) Protein expression levels of ERK, p-ERK, JNK, p-JNK, p38, p-p38 were determined by western blot. (B) Quantification of (A). ***P<0.001. (C) After BMMSCs were cultured with pathway inhibitors, protein

expression levels of ERK, p-ERK, JNK, p-JNK, p38, p-p38 were determined by western blot. (D) Quantification of (C). ***P<0.001. (E) Protein expression levels of OCN, OSX, RUNX2, ALP, OPN and COL-I were determined by western blot. (F) Quantification of (E). *P<0.05, **P<0.01, and ***P<0.001. (G) mRNA expression levels of OCN, OSX, RUNX2, ALP, OPN and COL-I were determined by qRT-PCR. **P<0.01, and ***P<0.001. (H) ALP staining on the 5th day. Scale bars=100 μm.

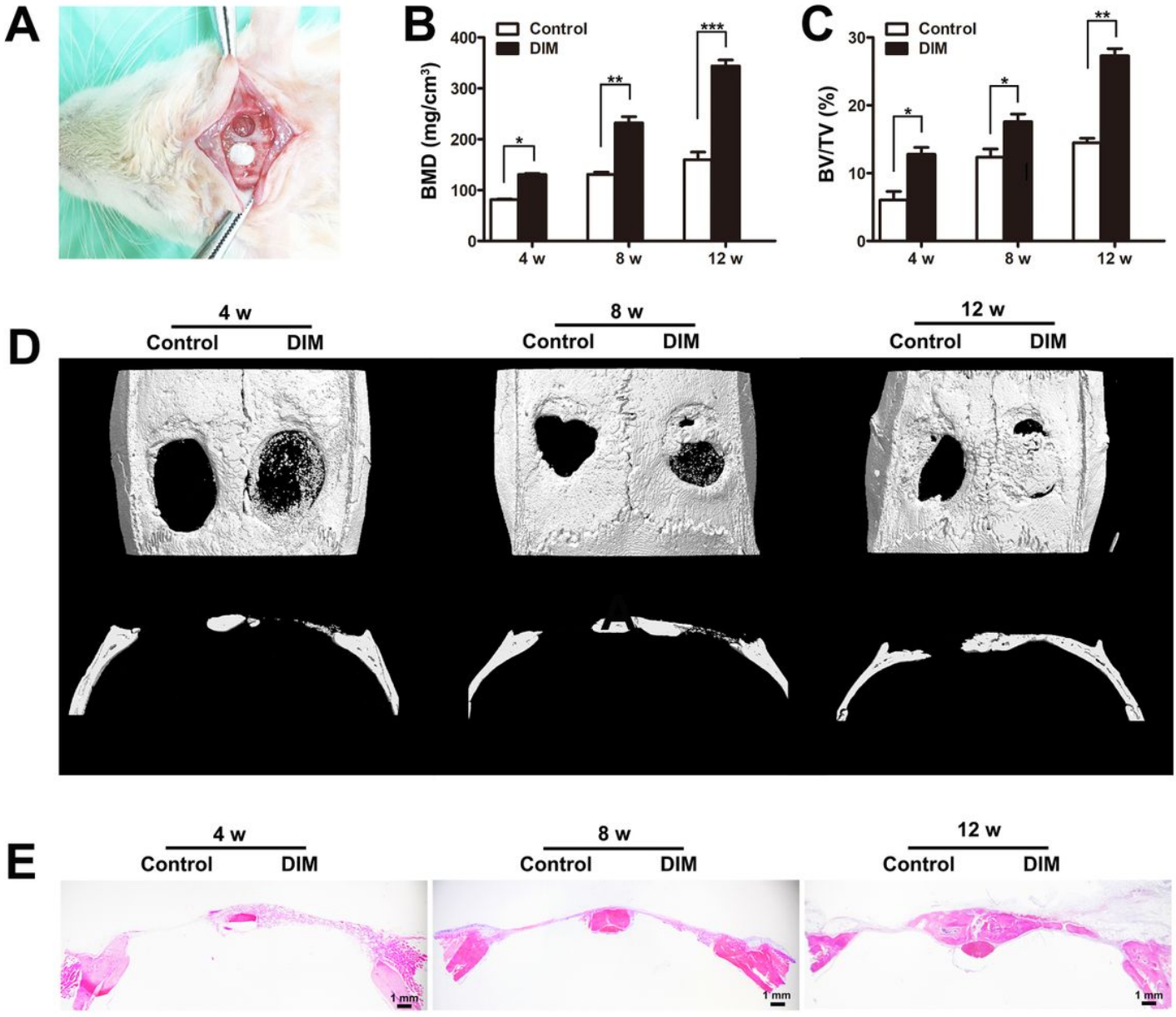

Figure 5

Micro-CT and H&E staining analysis of bone defects treated with DIM at 4, 8 and 12 weeks post-surgery (A) Image of a rat critical-sized calvarial defect model and DIM implantation. (B) Relative 3D reconstruction parameter BV/TV of newly formed bone by Micro-CT. *P<0.05, **P<0.01, and ***P<0.001. (C) Relative 3D reconstruction parameter BMD of newly formed bone by Micro-CT. *P<0.05, and **P<0.01. (D) 3D reconstruction of calvarial defects and exemplary axial sections by Micro-CT. (E) Representative coronal images of calvarial defects by H&E staining. Scale bars=1 mm.

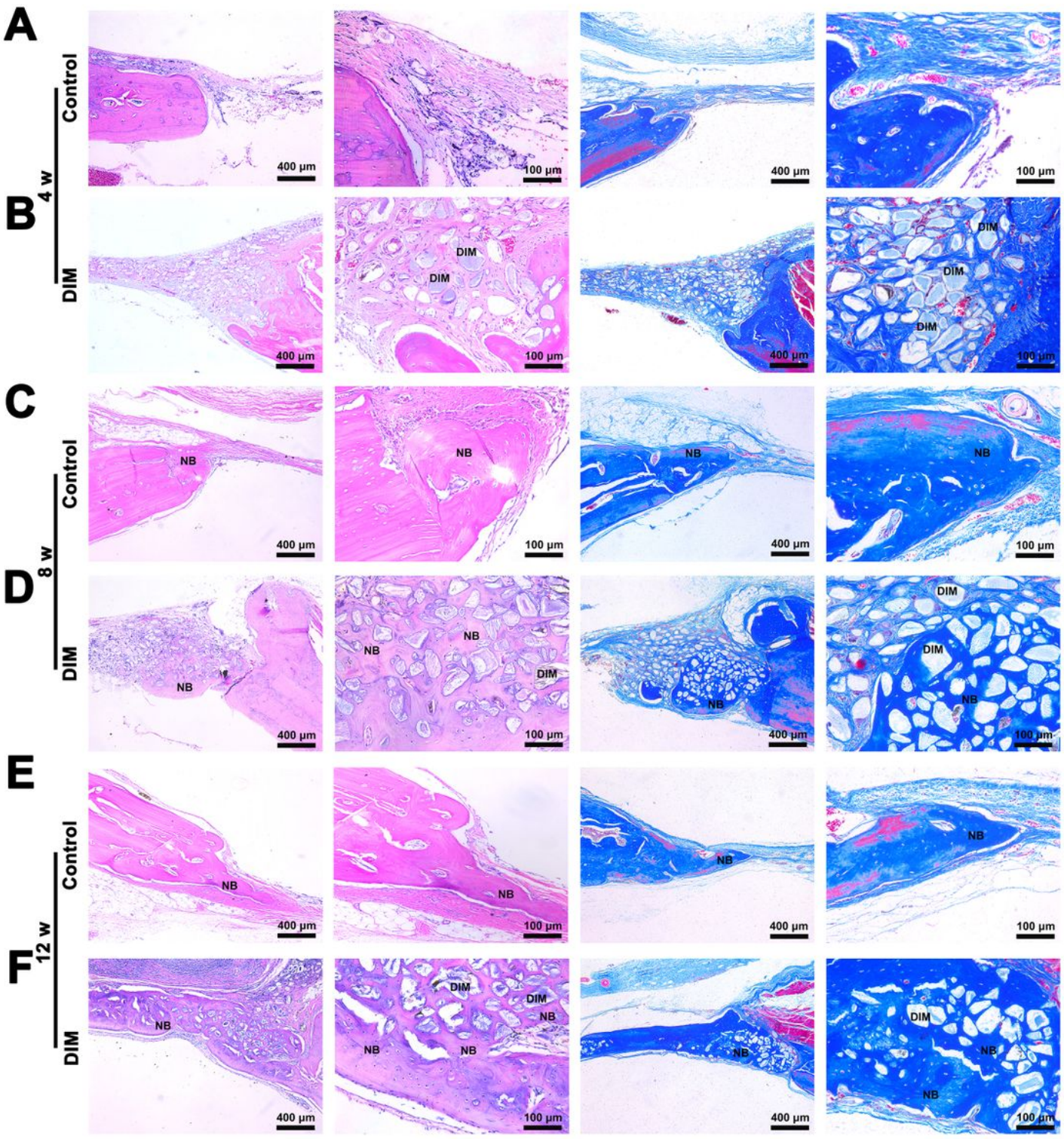

Figure 6

H&E and Masson's trichrome staining analysis of bone defects treated with DIM at 4, 8 and 12 weeks post-surgery (A, B) Coronal images of bone defects in DIM implantation and the control group after 4 weeks. (C, D) Coronal images of bone defects in DIM implantation group and the control group after 8 weeks. (E, F) Coronal images of bone defects in DIM implantation group and the control group after 12 weeks. DIM represent the residual material embedded in new bone. NB represent the newly formed bone.